Molecular Engineering of an Alkaline Naphthoquinone Flow Battery

Liuchuan Tong, Marc-Antoni Goulet, Daniel P. Tabor, Emily F. Kerr, Diana De Porcellinis, Eric M. Fell, Alán Aspuru-Guzik, Roy G. Gordon,* and Michael J. Aziz*

Dr. Liuchuan Tong, Dr. Daniel P. Tabor, Dr. Alán Aspuru-Guzik, Dr. Roy G. Gordon
Department of Chemistry and Chemical Biology, Harvard University, 12 Oxford Street, Cambridge, Massachusetts 02138, USA

Dr. Marc-Antoni Goulet, Dr. Diana De Porcellinis, Eric M. Fell, Dr. Michael J. Aziz
Harvard John A. Paulson School of Engineering and Applied Sciences, 29 Oxford Street, Cambridge, Massachusetts 02138, USA

Present Addresses
Dr. Marc-Antoni Goulet
Form Energy Inc.*,* Somerville, Massachusetts 02143, United States
Dr. Alán Aspuru-Guzik
Department of Chemistry and Department of Computer Science; Vector Institute for Artificial Intelligence, University of Toronto, Toronto, Ontario, M5S 1A1, Canada

*Corresponding authors:

Roy G. Gordon
Cabot Professor
Dept. of Chemistry and Chemical Biology
Harvard University
12 Oxford Street, MA 02138, USA
Tel: +1 617-495-4017
Fax: +1 617-495-4723
email: Gordon@chemistry.Harvard.edu

Michael J. Aziz
Gene and Tracy Sykes Professor of Materials and Energy Technologies
Harvard John A. Paulson School of Engineering and Applied Sciences, Pierce Hall 204a
29 Oxford Street, MA 02138, USA
Tel: +1 (617) 495-9884
email: maziz@harvard.edu

Table of Contents

Synthesis of bislawsone

The synthesis was carried out according to literature[1] with modifications.

Bislawsone, 2,2'-Bi(3-hydroxy-1,4-naphthoquinone). 2-hydroxynaphthoquinone (6.35 g, 36.46 mmol) and ammonium persulfate (16.64 g, 72.92 mmol) were dissolved in 240 mL of acetonitrile and water mixture (1:1 v/v) and refluxed for three hours at 80 °C. 20 mL glacial acetic acid was added to the cooled mixture before filtration to obtain a yellow solid (5.68 g, 45% yield). Additional acetic acid wash may be employed if NMR of the product showed the presence of impurities. ^{1}H NMR (500 MHz, DMSO-d$_6$): 8.10 (2H, d), 8.01 (2H, d), 7.86 (4H, m). ^{13}C NMR (125 MHz, DMSO-d6): 182.30, 180.19, 156.41, 134.96, 133.56, 132.06, 130.18, 126.13, 125.98, 115.50

Electrochemical Characterization

Cyclic Voltammetry (CV) and Rotating Disk Electrode (RDE) Measurements

Glassy carbon was used as the working electrode for all three-electrode CV tests. RDE experiments were conducted using a Pine Instruments Modulated Speed Rotator AFMSRCE equipped with a 5 mm diameter glassy carbon working electrode, a Ag/AgCl reference electrode (BASi, pre-soaked in 1 M KCl solution), and a graphite counter electrode. The electrode was rotated at a specific speed while the voltage was linearly swept from -0.4 to -1.4 V *vs* Ag/AgCl (a). The diffusion coefficient of the oxidized form of bislawsone was calculated using the Levich equation, which relates the mass transport-limited current to the number of electrons transferred (n), the area of the electrode (A), and the concentration of redox-active species in the electrolyte (C), by plotting the mass-transport-limited current against the square root of the rotation rate (b), with the following parameters: $n = 4$, F = 96,485 Coulombs/mol, $A = 0.196$ cm^2, $C = 5$ mM, kinematic viscosity of 1 M KOH, $v = 1.08 \times 10^{-6}$ m^2/s. The resulting value of the diffusion coefficient for the oxidized form of bislawsone is 4.54×10^{-6} cm^2/s.

Permeability Measurement

The permeability of the oxidized form of lawsone and bislawsone across a Fumasep E-620K membrane was evaluated with a lab-made two-compartment cell. The donating side was filled with a solution of lawsone or bislawsone (0.05 M) in 1 M KOH, while the receiving side was filled with 0.024 M KCl in 1 M KOH to balance the osmotic pressure . Both compartments had the same volume. The solutions were continuously mixed by keeping the cell on a nutating table. At different time intervals, aliquots were taken from the receiving side, diluted, characterized by UV-Vis spectrophotometry and replaced by fresh KOH solution. The concentration was calculated from a calibration curve and the permeability of lawsone and bislawsone was calculated based on Fick's law using the following equation:

$$P = \frac{\Delta ln(1 - \frac{2c_t}{c_0})(-\frac{V_o l}{2A})}{\Delta t}$$

where P is permeability coefficient [cm^2/s], A is the effective membrane area [cm^2], t is elapsed time [s], c_t [mol/L] is the concentration of active species in the receiving side at time t, Vo is the volume of the solution in either compartment (5 cm^3), l is the thickness of the membrane

($\sim$ 20 μm), c_o is the concentration of lawsone or bislawsone in the donating side at time zero (0.05 mol/L), and Δ represents a finite difference.

Full Cell Measurements

Flow cells were constructed similar to a previous report.[2-3] Pyrosealed POCO graphite flow plates with serpentine flow patterns were used for both electrodes. Each electrode comprised a 5 cm² geometric surface area covered by a stack of three or four sheets of Sigracet SGL 39AA porous carbon paper pre-baked in air overnight at 400 °C. A Fumasep E-620K membrane served as the ion-selective membrane between the carbon electrodes. The electrolyte was pumped at 60 mL/min controlled by Cole-Parmer Masterflex L/S peristaltic pumps. All cells were run inside a nitrogen-filled glove bag, and cell polarization and charge-discharge cycling were performed using a Biologic VSP 300 potentiostat.

For low concentration (0.1 M) full cell measurement, the posolyte volume was 44 mL and its composition, when assembled, was 0.20 M potassium ferrocyanide, 0.02 M potassium ferricyanide and 1 M KOH. The negolyte was prepared by dissolving 0.1 M bislawsone in its oxidized form in 1.2 M KOH solution resulting in 8 mL 0.1 M bislawsone and 1.2 M K^+ and 1 M OH^- electrolyte solution.

For high concentration (0.5 M) full cell measurement, the posolyte volume was 95 mL and its composition, when assembled, was 0.30 M potassium ferrocyanide, 0.10 M potassium ferricyanide and 1 M KOH. The negolyte was prepared by dissolving 0.5 M bislawsone in its fully oxidized form in 2.0 M KOH solution resulting in 8 mL 0.5 M bislawsone and 2 M K^+ and 1 M OH^- electrolyte solution for Figure 3A, 3B, 3C, and 6 mL 0.5 M bislawsone and 2 M K^+ and 1 M OH^- electrolyte solution for Figure 3D.

Galvanostatic cycling was performed at ±0.1 A/cm² at room temperature, with voltage limits and holds of 0.5 and 1.4 V until currents drop below 2 mA/cm². To obtain the polarization curves, the cell was first charged to the desired state of charge, and then polarized via linear sweep voltammetry at a rate of 100 mV/s. For high concentration 0.5 M bislawsone cell, ±0.3 A/cm² current was applied after the initial 12.6 days of cycling at ±0.1 A/cm².

High-resolution LC-MS and preparative HPLC experiments

High-resolution LC-MS analysis of electrolyte was performed in the Small Molecule Mass Spectrometry Facility at Harvard on a Bruker Impact II q-TOF with internal calibration sodium formate clusters. Liquid chromatography was performed on an Agilent 1290 Infinity HPLC using a Allure PFPP column (5 μm particle size, 150 x 2.1 mm) at a flow rate of 0.4 mL/min and the following elution conditions were applied (solvent A = 0.1% v/v formic acid in water; solvent B = 0.1% v/v formic acid in acetonitrile): 95% solvent A for 2 min, a gradient increasing from 5% to 60% solvent B in solvent A over 13 min, a gradient increasing to 100% solvent B over 5 min, a gradient decreasing to 5% solvent B in solvent A over 0.1 min, and 100% solvent A for 4.9 min. The ESI mass spectra were recorded in negative ionization mode.

Preparative HPLC was performed using a Thermo Scientific Hypersil GOLD aQ column (5 μm particle size, 250 x 20 mm) at a flow rate of 10 mL/min and the following elution conditions were applied (solvent A = 0.1% v/v formic acid in water; solvent B = 0.1% v/v formic acid in acetonitrile): 80% solvent A for 2 min, a gradient increasing from 20% to 70% solvent B in

solvent A over 5 min, a gradient increasing to 85% solvent B over 10 min, a gradient increasing to 95% solvent B over 4 min, a gradient decreasing to 20% solvent B in solvent A over 1 min, and 20% solvent B for 2 min. The eluent fractions were collected and lyophilized for subsequent LC-MS confirmation

Theoretical Calculations

We calculated the properties of a library of lawsone-derived molecules in order to gain some understanding for the increased stability of bislawsone relative to lawsone and identify candidates that may have superior performance to bislawsone. The results of the full library are provided in the supplementary spreadsheet. The primary modifications include varying the number of carbon atoms between the lawsone units and the functional groups attached to the benzene ring. Functional groups considered include hydroxyl, methoxy, ethoxy, methyl, ethyl, CH_2-CH_2-OH, amine, and the oxy-butyrate functional group (with the number of carbons varied) employed in 2-6 DBEAQ.

For the calculations, the molecules are left in their neutral forms to reduce errors associated with calculating the energies of anions. This leads to a slightly overestimation of the reduction potentials, but the overestimation is mostly systematic and by looking at differences we can capture all of the relevant structure-property relationships. Energetics are evaluated at the B3LYP/6-311+G(d,p) (PCM) level of theory.

The calculated thermodynamic susceptibility of the reduced forms of bislawsone tautomerizing to the partially redox inactive forms is shown in Figure 4A. These calculated reaction energies are over 0.1 eV higher than the analogous tautomerization energy for lawsone (0.02 eV), indicating that forming this dimer mitigates the effects of this decomposition mechanism. The calculations also predict that the half-reduced (2e⁻ reduced) form is more susceptible to tautomerization than the fully reduced form (4e⁻ reduced).

Within the set of 193 bislawsone derivatives, we found 8 derivatives that are predicted to be more stable than bislawsone (against both "type 1" and "type 2" decomposition) and have reduction potentials within 0.1V of bislawsone. This set of molecules is shown in Figure S16. Examining these molecules, we see a variety of viable derivatives that vary the number of carbon atoms between the lawsone subunits (up to 3) but see a common pattern in the functional groups that are predicted to increase stability. These alkyl groups terminated by an alkyoxy group on one end and a carboxylic acid group are emerging as common motifs in stabilized anthraquinone flow battery molecules. One molecule, with a two-carbon linkage between the lawsone units, and 4 total functionalizations (of the -OCCCOOH type) is predicted to be both more stable and lower in reduction potential (by about 0.04 V) than bislawsone.
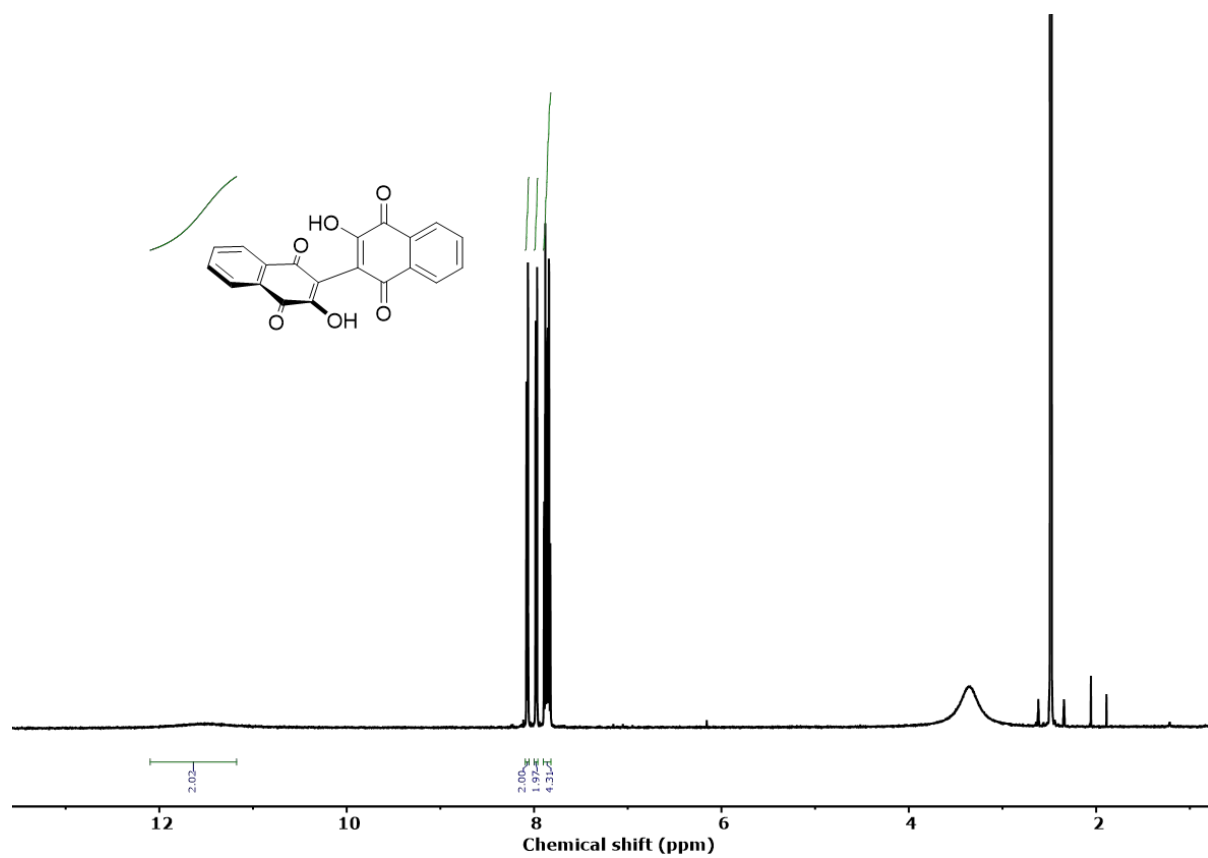
Figure S1

Figure S1 1H NMR spectrum of bislawsone in DMSO-d6. ^{1}H NMR (500 MHz, DMSO-d6) δ: 11.51 (br, 2H), 8.07 (d, 2H), 7.97 (dd, 2H), 7.90-7.82 (m, 4H).
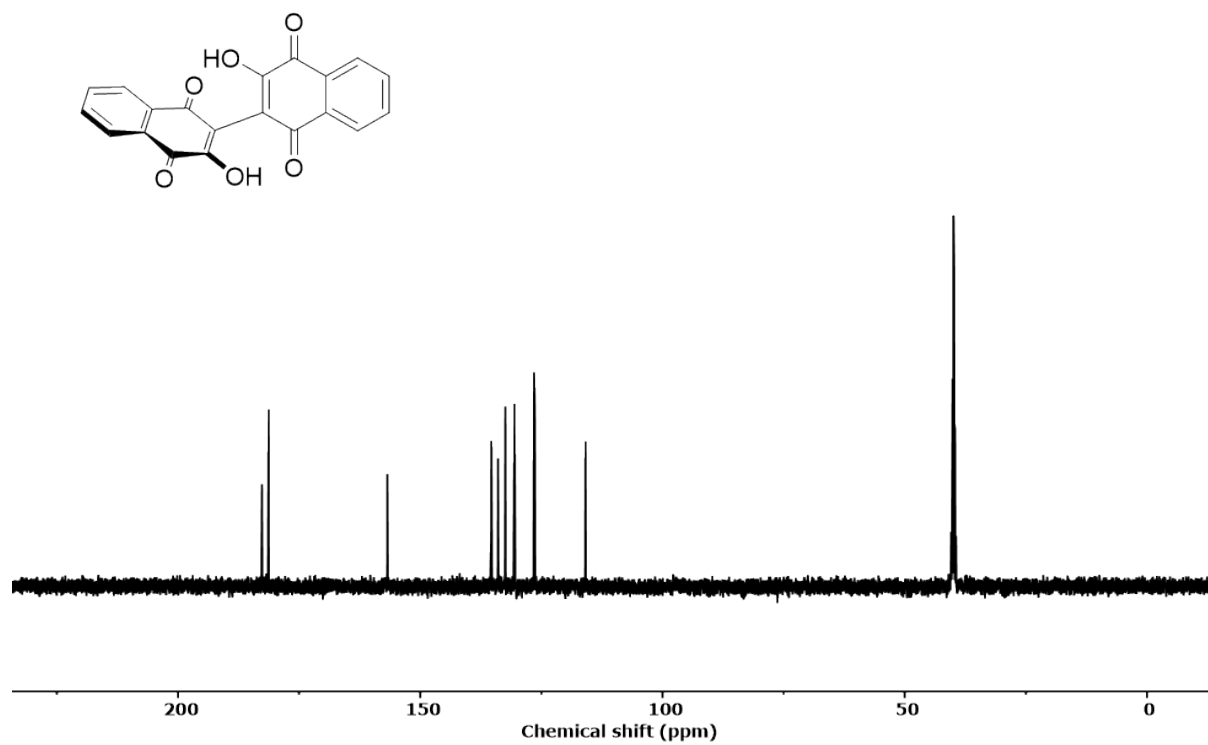
Figure S2

Figure S2 ¹³C NMR spectrum of bislawsone in DMSO-d6. ¹³C NMR (125 MHz, CDCl3) δ:
182.68, 181.29, 156.79, 135.33, 133.94, 133.44, 130.56, 126.51, 126.36, 115.89.
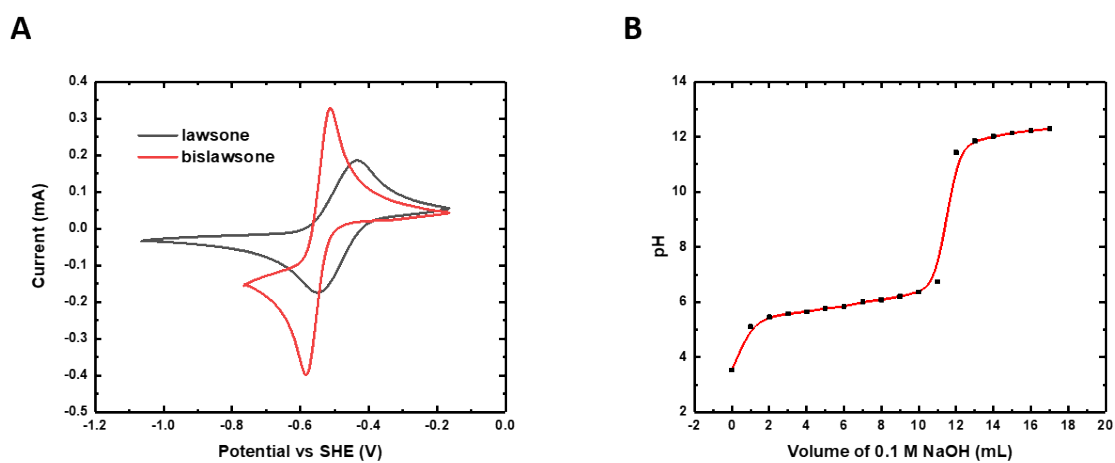
Figure S3

Figure S3. (A) Cyclic voltammograms of 5 mM bislawsone (red), and 5 mM lawsone (black) in 1M KOH at a scan rate of 50 mV/s. (B) Titration of 10 mL 0.1M lawsone with 0.1 M NaOH solution

Table S1 Comparison of bislawsone with lawsone.

	Reduction potential (vs SHE in 1M KOH)	Solubility	pKa	Permeability
lawsone	-0.501 V	0.48 M	6.0	1.01×10^{-10} cm^2/s
bislawsone	-0.551 V	0.56 M	6.5	1.19×10^{-11} cm^2/s

8
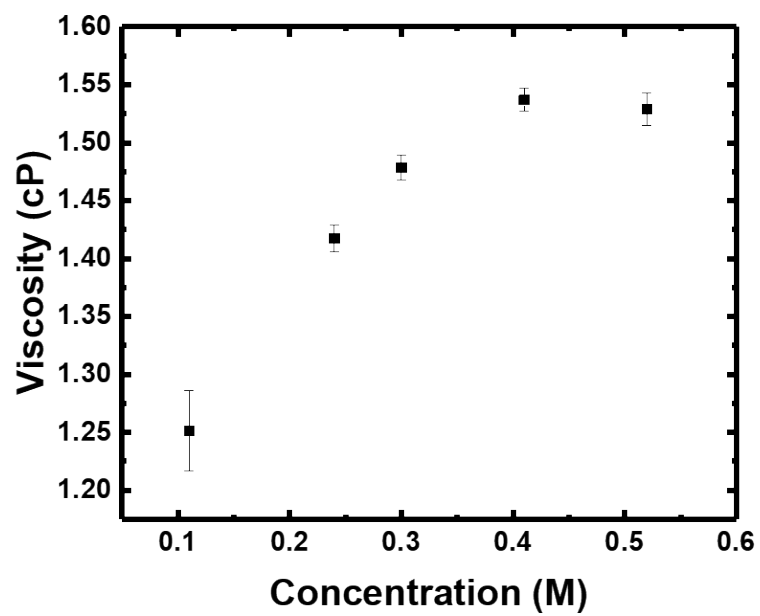
Figure S4

Figure S4. Viscosity measurement of bislawsone at various concentration in 1M KOH

Figure S5
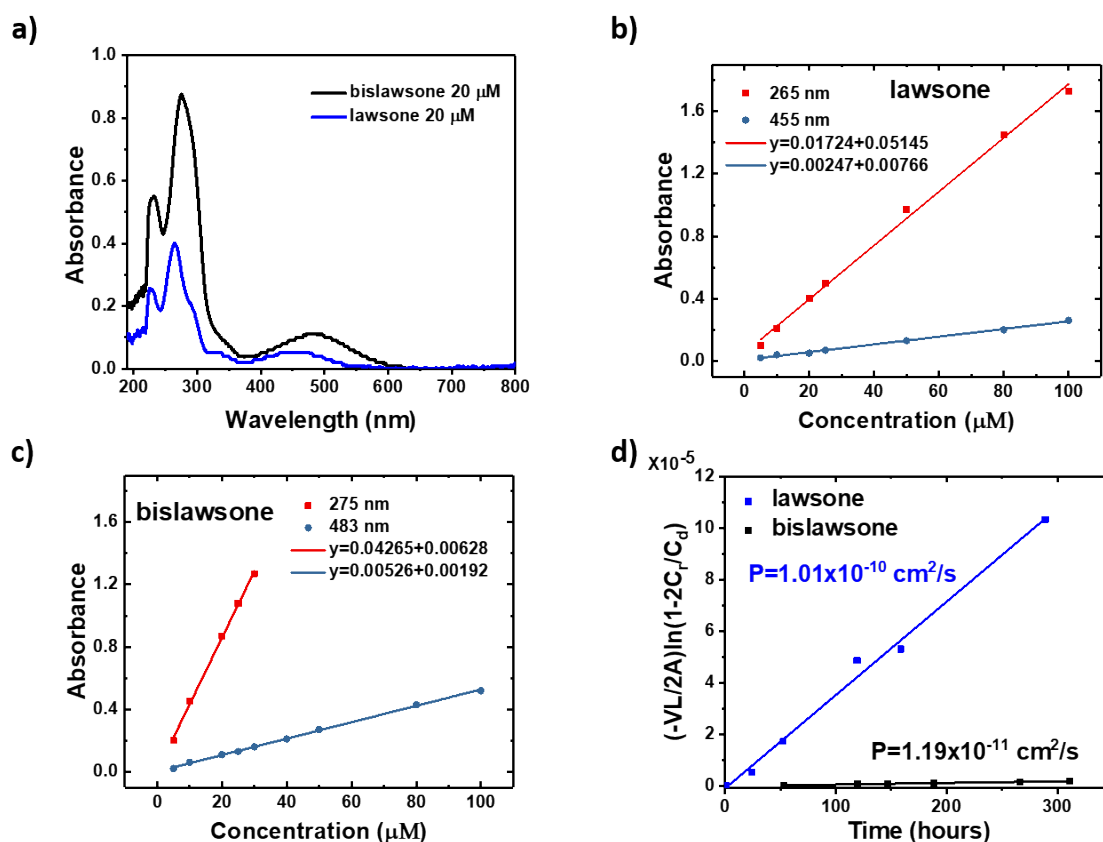
Figure S5. (a) Representative UV-Vis spectrum of lawsone and bislawsone at 20 μM in 1M KOH. (b) Calibration curve of lawsone in 1 M KOH. Peaks at 265 and 455 nm were selected for calibration. (c) Calibration curve of bislawsone in 1 M KOH. Peaks at 275 and 483 nm were selected for calibration. (d) Comparison of permeability of lawsone and bislawsone in 1 M KOH through Fumasep E-620K based on crossover test.

Figure S6
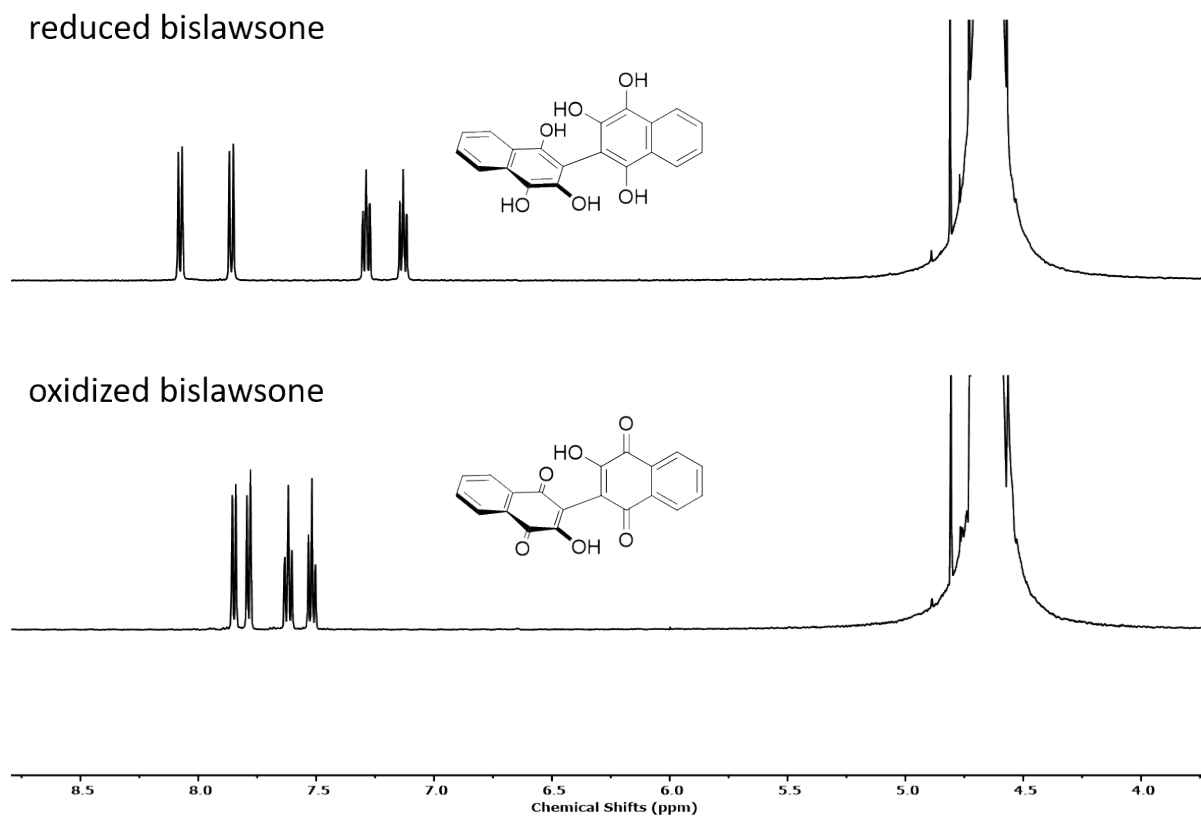
Figure S6 ^{1}H NMR spectrum of fully reduced bislawsone (top) and oxidized bislawsone (bottom) in D$_2$O/KOH solution after 3 cycles. Reduced bislawsone: ^{1}H NMR (500 MHz, CDCl$_3$) δ: 8.07 (d, 2H), 7.86 (d, 2H), 7.28 (dd, 2H), 7.13 (dd, 2H). Oxidized bislawsone: ^{1}H NMR (500 MHz, CDCl$_3$) δ: 7.85 (d, 2H), 7.78 (d, 2H), 7.62 (dd, 2H), 7.52 (dd, 2H).

Figure S7
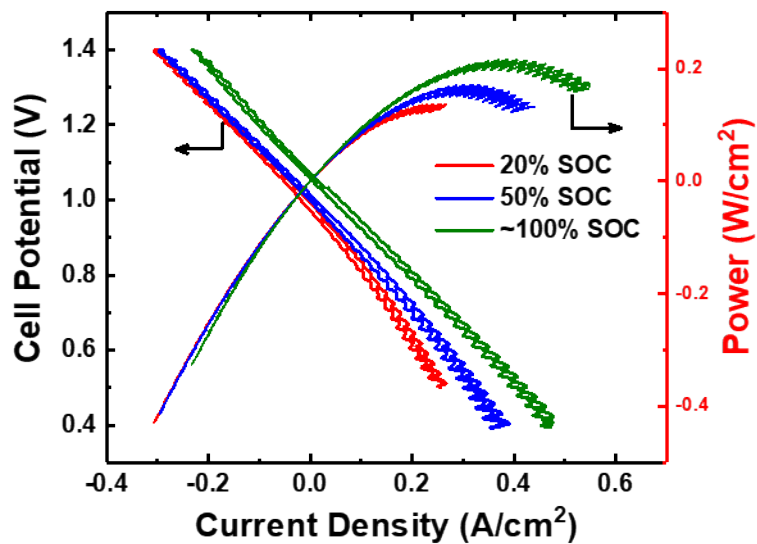
Figure S7 Electrochemical performance of a 0.1 M bislawsone/K$_4$Fe(CN)$_6$ cell. The cell-polarization plots, composed of cell potential (left vertical) and power density (right vertical) versus current density.

Figure S8
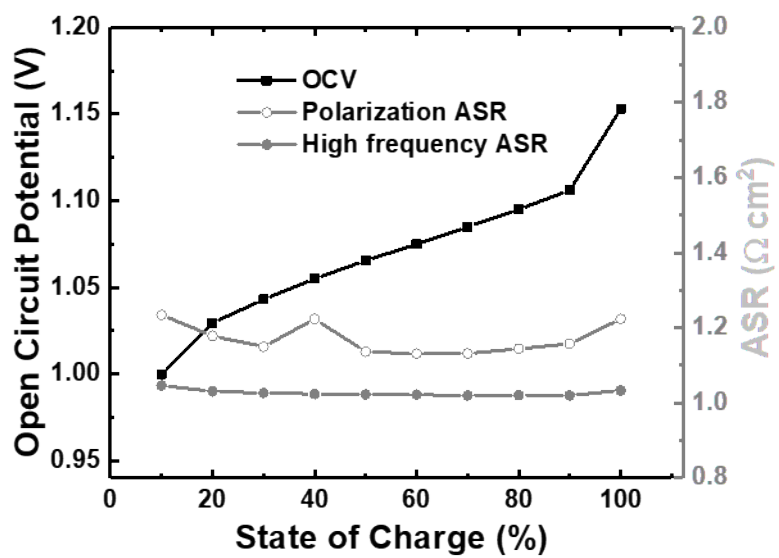
Figure S8. OCV, high-frequency, and polarization ASR versus SOC of 0.5 M bislawsone cell

Figure S9
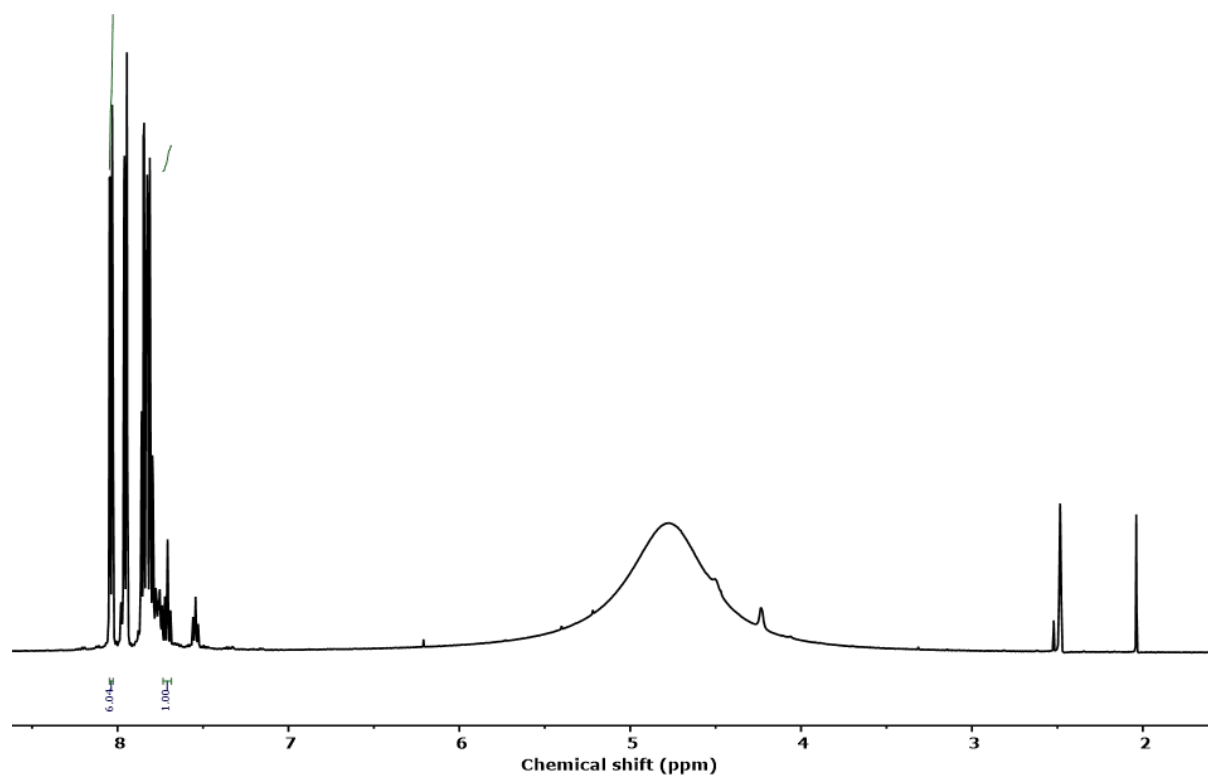
Figure S9. NMR spectrum of cycled bislawsone in DMSO after acidified with HCl.

Figure S10
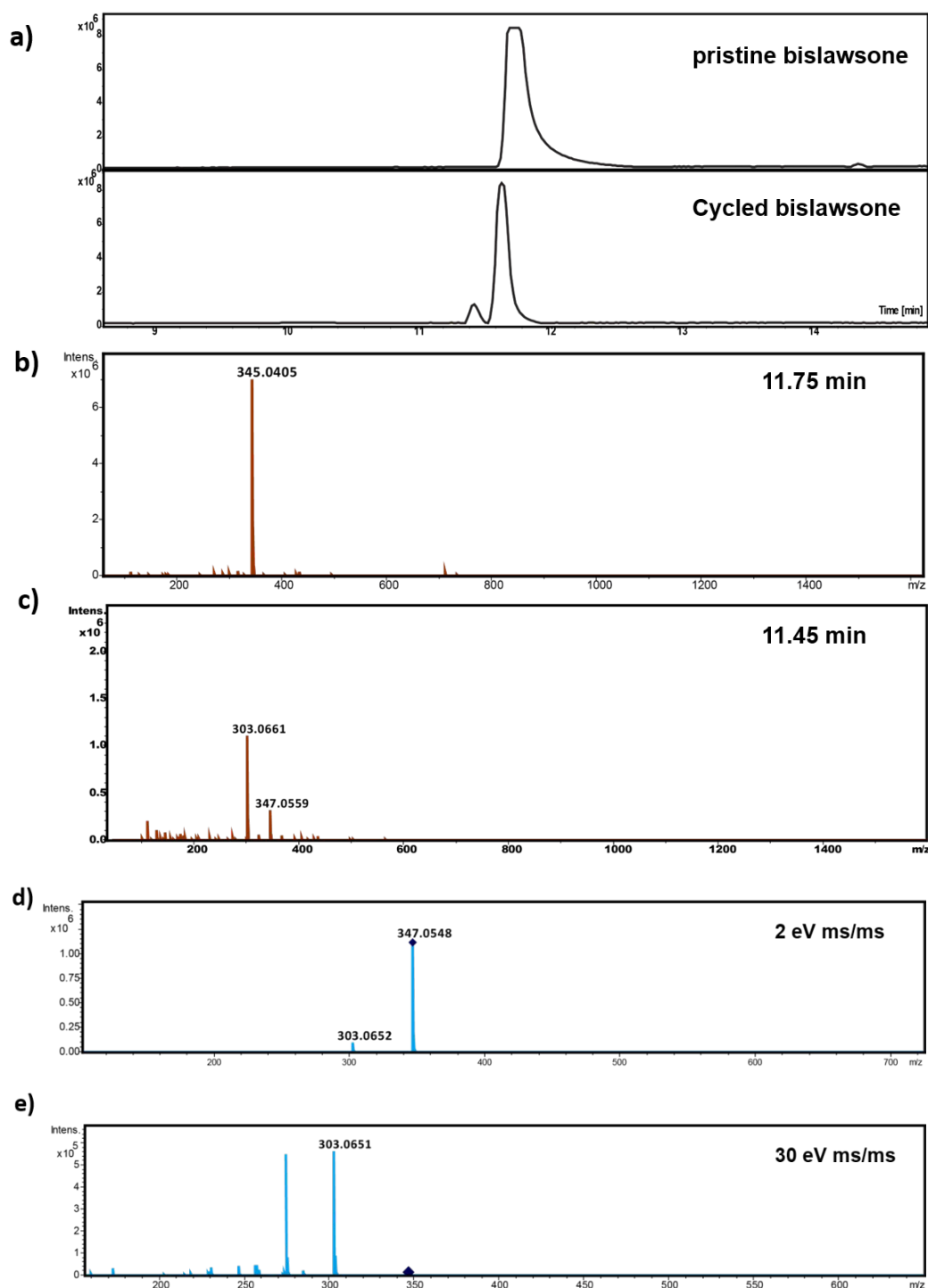
Figure S10 **High-resolution liquid chromatograph mass spectrometry.** (a) LC-MS of pristine bislawsone (top) and a bislawone sample that has been cycled for 21 days (bottom). (b) Mass spectrum of cycled sample at 11.75 min showing the major peak is bislawsone (m/z = 345.0405). (c) Mass spectrum of cycled sample at 11.45 min showing the degradation product m/z of 347.0559, and fragment m/z of 303.0661. (d) Tandem LC-MSMS of m/z 347.0548 at minimal 2 eV shows that minimal fragmentation occurred. (e) Tandem LC-MSMS of m/z 347.0548 at high 30 eV shows that most of the parent ion fragmented into m/z = 303.0651. This result confirms that m/z = 303.0651 signal is a fragment of parent m/z = 347.0548 instead

of an independent species that is coeluting. The diamond symbol indicates the target mass for fragmentation.

Figure S11
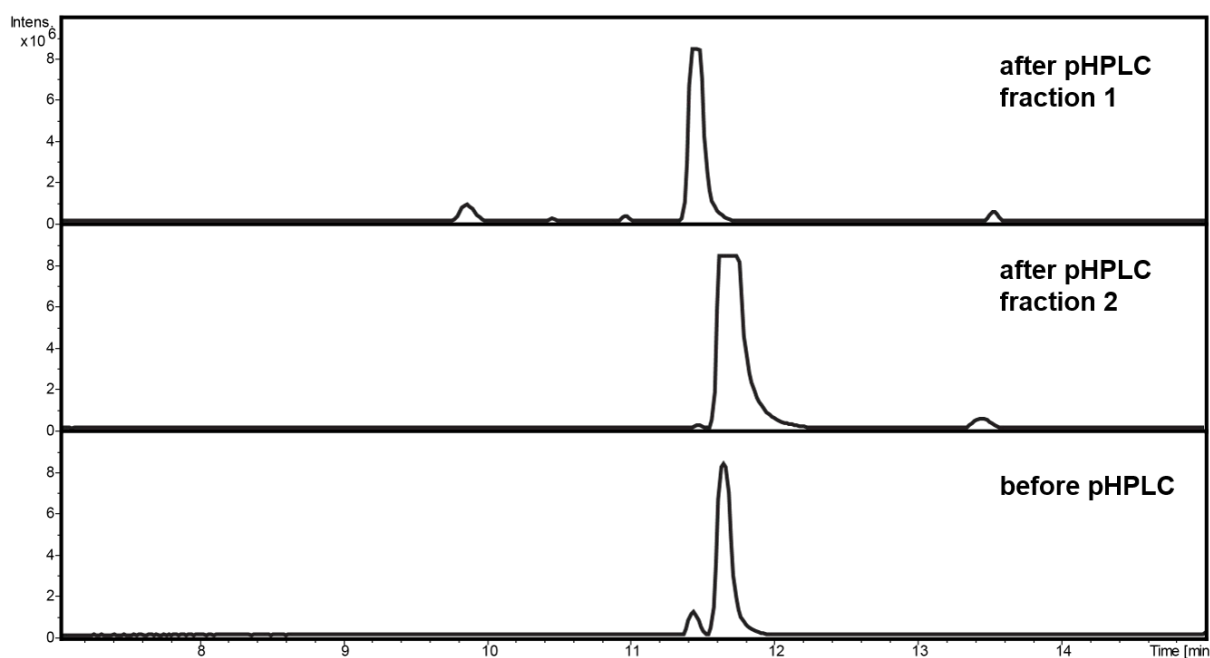
Figure S11. **LC-MS of Fractions Collected from Preparative High-Performance Liquid Chromatography Separation** LC-MS traces showing cycled bislawone mixture before pHPLC separation(bottom), purified bislawsone fraction at 11.75 min (middle), and purified degradation product at 11.45 min. This result showed that the degradation product can be purified from cycled electrolyte mixture for structure identification. The small peaks at 10 min and 13.5 min are impurities from pHPLC columns and do not affect subsequent NMR analysis.
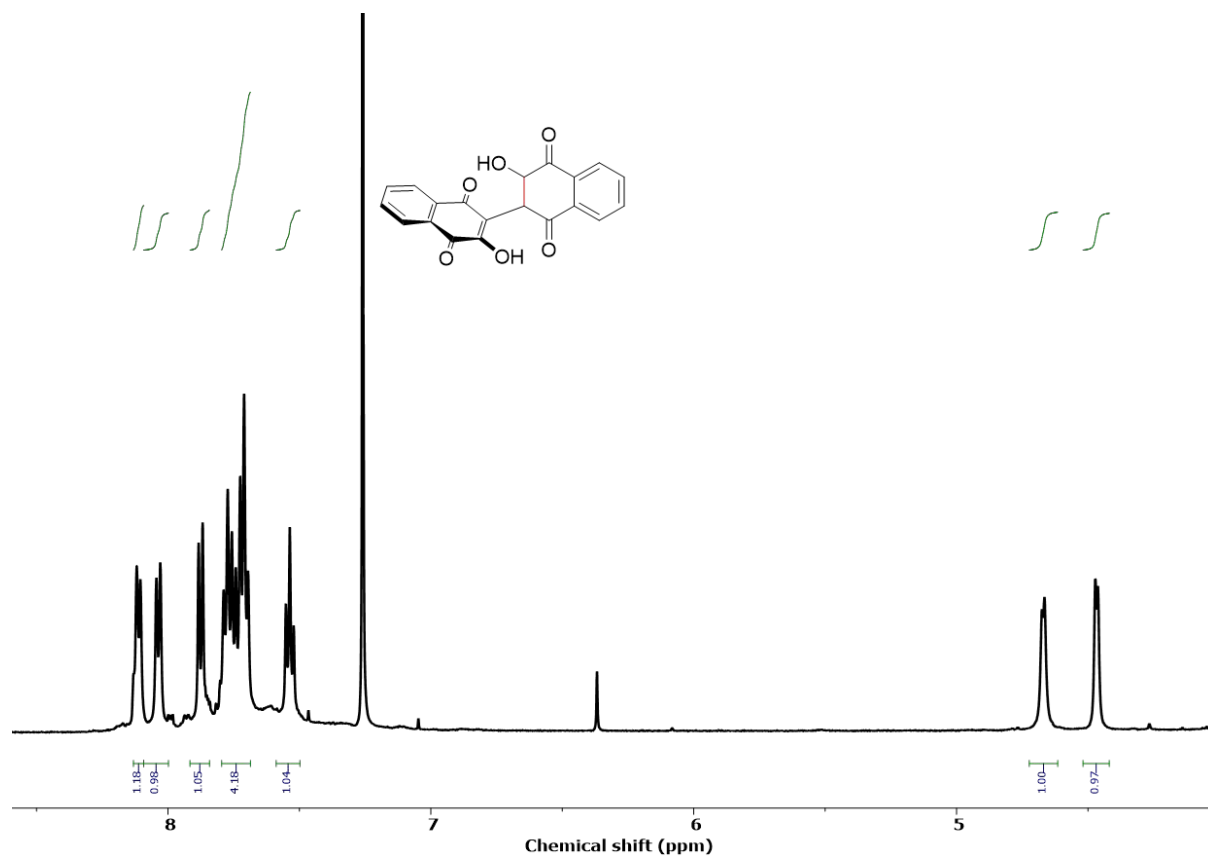
Figure S12. **1H NMR spectrum of degradation product 2,3-dihydrobislawsone**. ^{1}H NMR (500 MHz, CDCl$_3$) δ: 8.12 (d, 1H), 8.04 (d, 1H), 7.88 (d, 1H), 7.80-7.68 (m, 4H), 7.54 (dd, 1H), 4.67 (d, 1H), 4.47 (d, 1H). The presence of inter-splitting aliphatic proton indicates the presence of carbon-carbon single bond.
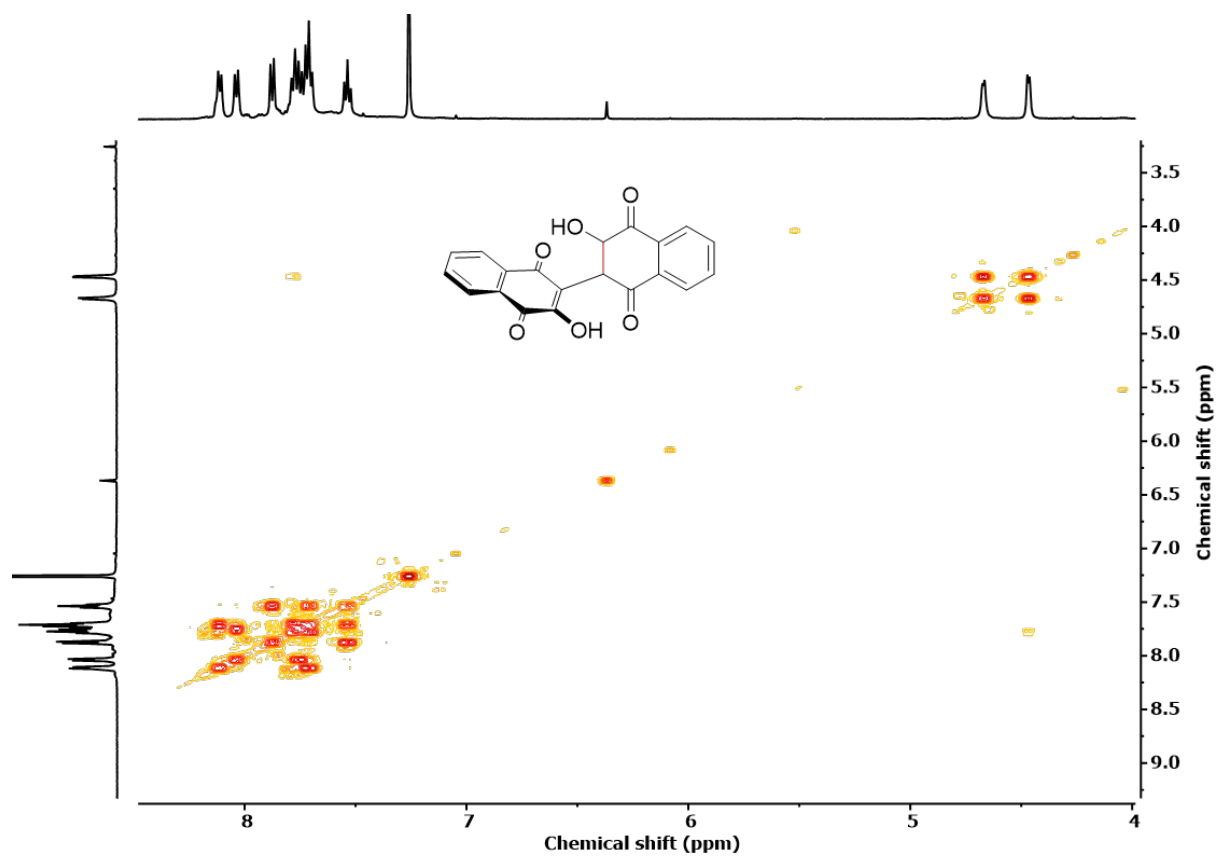
Figure S13

Figure S13. **COSY NMR spectrum of degradation product 2,3-dihydrobislawsone**. Two aliphatic protons split each other.
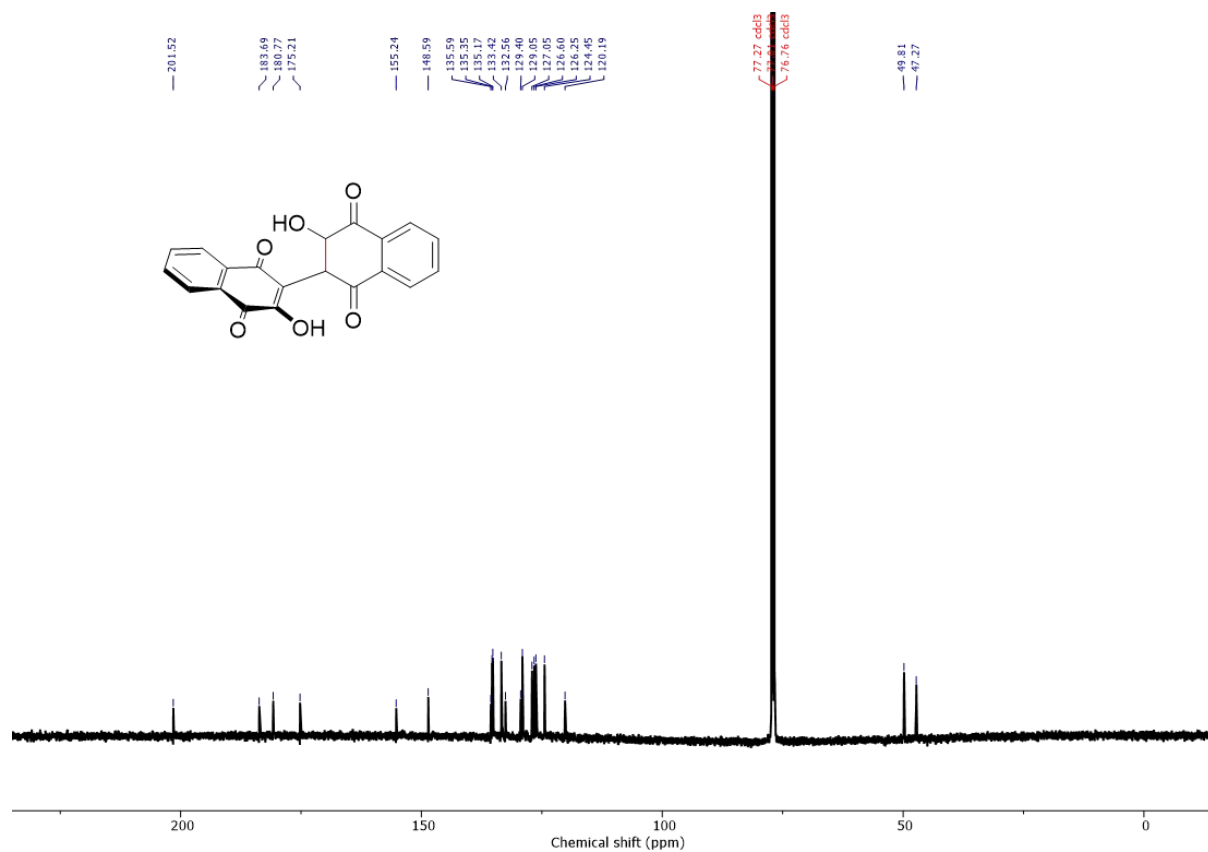
Figure S14

Figure S14. **¹³C NMR spectrum of degradation product 2,3-dihydrobislawsone**. ¹³C NMR (125 MHz, CDCl3) δ: 201.5, 183.69, 180.77, 175.21, 155.24, 148.59, 135.59, 135.35, 135.17, 133.42, 132.56, 129.40, 129.05, 137.05, 126.60, 126.25, 124.45, 120.19, 49.81, 47.27. A total of 20 distinct carbon peaks indicate the asymmetry of the structure.
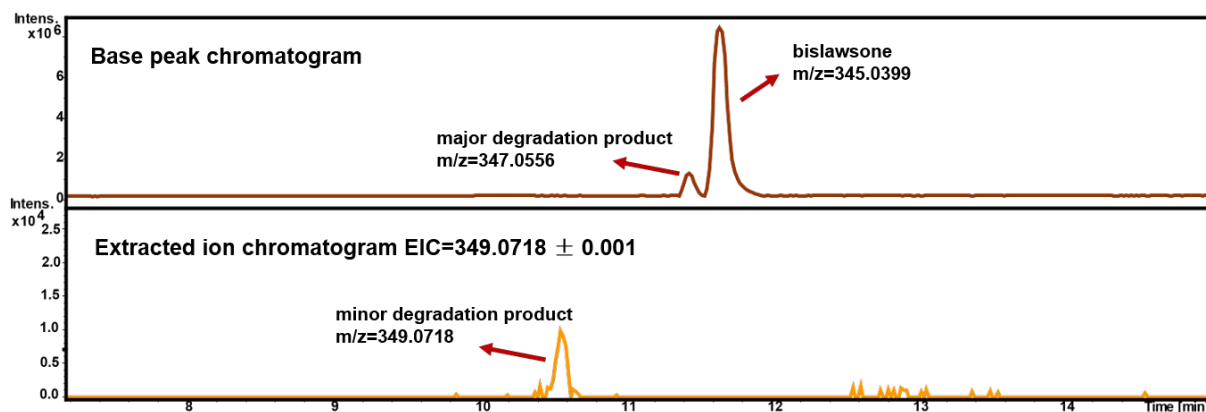
Figure S15

Figure S15. **LC-MS detection of redox-inactive 2,2`,3,3`-tetrahydrobislawsone.** Top) Base peak chromatogram of 0.5 M bislawsone cell cycled for 21 days showing bislawsone peak at 11.7 min and 2,3-dihydrobislawsone peak as major degradation product at 11.4 min. Bottom) Extracted ion chromatogram of 349.0718 ± 0.001 showing the minor degradation product in around 1% concentration.
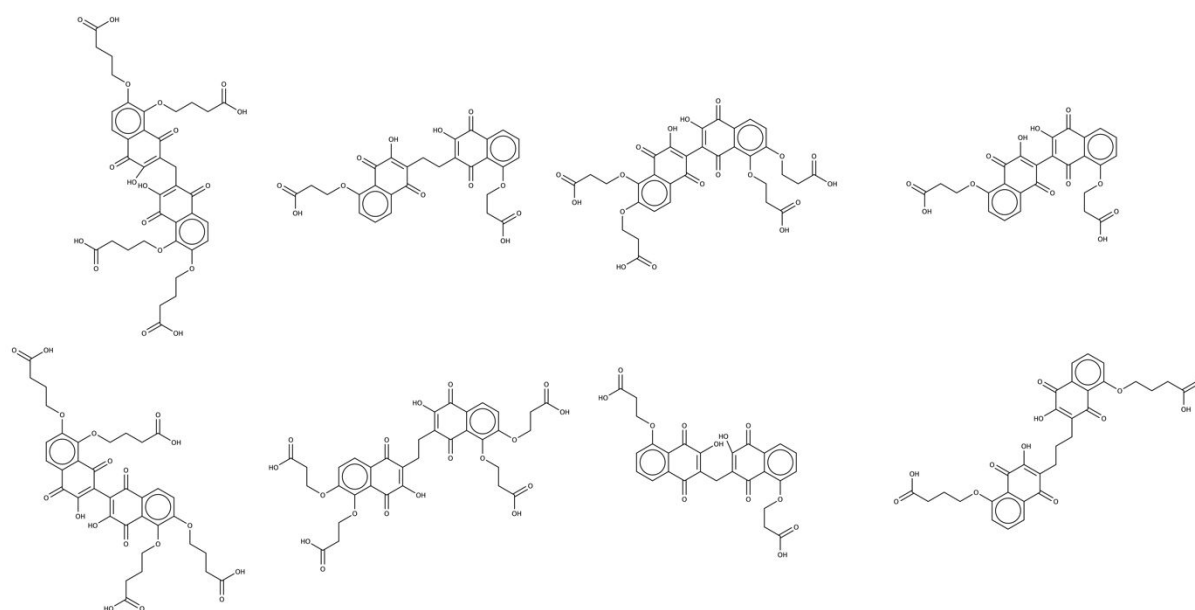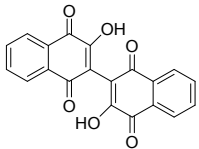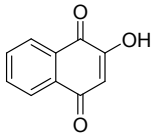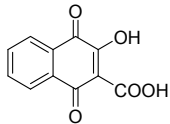
Figure S16
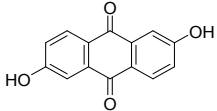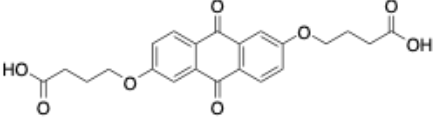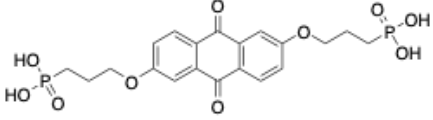
Figure S16. Predicted Stable Molecules. These molecules are bislawsone derivatives that are predicted to have two-proton-two-electron reduction within 0.1 V of bislawsone for each of the reduction reactions and are less thermodynamically susceptible to tautomerization than bislawsone. All energies (B3LYP/6-311+G(d,p) PCM) are provided in supplementary spreadsheet.
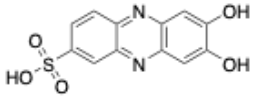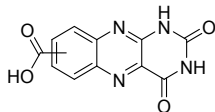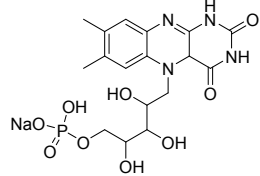
Table S2. Overview of reported high performance negolytes for alkaline organic flow battery (at pH 14 unless otherwise noted).

Negative electrolyte	Potential (V vs.SHE)	Solubility	# of electrons	Capacity loss per day
Bislawsone (This work)	-0.55	0.56 M	4	0.75%
2-hydroxy-1,4-naphthoquinone (lawsone)[4]	-0.49	0.48 M	2	4.1%
2-hydroxy-3-carboxyl-1,4-naphthoquinone (2,3-HCNQ)[4]	-0.52	1.2 M	2	6.4%
2,6-dihydroxyanthraquinone (DHAQ)[3]	-0.68	0.6 M	2	est. 5.6%.

2,6-DBEAQ[2]

-0.52   1.1M / 0.6M (pH 12)   2   0.04% (pH 12)

2,6-DPPEAQ[5]

-0.47 (pH 9)   0.75M (pH 9)   2   0.014% (pH 9 - 12)

7,8-dihydroxyphenazine-2-sulfonic acid (DHPS)[6]

-0.85   1.8M   2   0.68%

alloxazine 7/8-carboxylic acid (ACA) [7]

-0.62   0.5 M   2   est. 0.93%

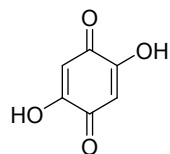riboflavin-5'-monophosphate sodium salt (FMN-Na) [8]

-0.52   0.24 M   2   0.52%
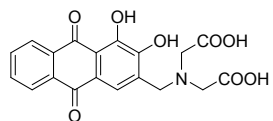
alizarin-3-methyliminodiacetic acid
(AMA) [9]

| | -0.67 | 0.4 M | 2 | 19.4% |

2,6-dihydroxybenzoquinone
(DHBQ)[10]

| | -0.72 | 4.31 M | 2 | est.9% |

Frequently Asked Questions

Q: Why was the Pourbaix diagram not measured?

A: We agree that the Pourbaix diagram offers insight into the proton and electron transfer processes of a redox system. However, bislawsone did not show a reversible CV signal in buffered solution from pH 12 to pH 2. The lack of reversible CV signal has also been observed in other alpha-hydroxy quinone systems 2,6-DihydroxyBenzoquinone (*Adv. Energy Mater.* 2018, **8**, 1702056). The exact origin of this phenomenon is unknown at this time.

Q: The initial Coulombic efficiency in Figure 2D is ~99%, but it rapidly increases to 99.5% at the time of 0.5 day. Why?

A: The cell was cycled in a nitrogen filled glovebag along with several other cells running in parallel in adjacent glovebags with the same nitrogen supply. The initial gradual increase in the Coulombic efficiency is due to a gradual depletion of dissolved oxygen gas in the electrolytes/cells which were prepared outside of the glove bag. The artifact of the ~0.5% jump in Coulombic efficiency at 0.5 day is most likely due to a sudden ramp in the nitrogen pressure or a better seal of the glove bag. Because the organic redox materials are sensitive to oxygen, we have observed this fluctuation in Coulombic efficiency in several cases where the nitrogen pressure was changed or a pinhole was created/sealed in the glovebag.

References

1. Inagaki, R.; Ninomiya, M.; Tanaka, K.; Koketsu, M., Synthesis, Characterization, and Antileukemic Properties of Naphthoquinone Derivatives of Lawsone. *ChemMedChem* **2015,** *10* (8), 1413-1423.

2. Kwabi, D. G.; Lin, K.; Ji, Y.; Kerr, E. F.; Goulet, M.-A.; De Porcellinis, D.; Tabor, D. P.; Pollack, D. A.; Aspuru-Guzik, A.; Gordon, R. G.; Aziz, M. J., Alkaline quinone flow battery with long lifetime at pH 12. *Joule* **2018,** *2*, 1907.

3. Lin, K.; Chen, Q.; Gerhardt, M. R.; Tong, L.; Kim, S. B.; Eisenach, L.; Valle, A. W.; Hardee, D.; Gordon, R. G.; Aziz, M. J.; Marshak, M. P., Alkaline quinone flow battery. *Science* **2015,** *349* (6255), 1529-32.

4.   Wang, C.; Yang, Z.; Wang, Y.; Zhao, P.; Yan, W.; Zhu, G.; Ma, L.; Yu, B.; Wang, L.; Li, G.; Liu, J.; Jin, Z., High-Performance Alkaline Organic Redox Flow Batteries Based on 2-Hydroxy-3-carboxy-1,4-naphthoquinone. *ACS Energy Letters* **2018,** *3* (10), 2404-2409.

5.   Ji, Y.; Goulet, M.-A.; Pollack, D. A.; Kwabi, D. G.; Jin, S.; De Porcellinis, D.; Kerr, E. F.; Gordon, R. G.; Aziz, M. J., A Phosphonate-Functionalized Quinone Redox Flow Battery at Near-Neutral pH with Record Capacity Retention Rate. *Advanced Energy Materials* **2019,** *9* (12), 1900039.

6.   Hollas, A.; Wei, X.; Murugesan, V.; Nie, Z.; Li, B.; Reed, D.; Liu, J.; Sprenkle, V.; Wang, W., A biomimetic high-capacity phenazine-based anolyte for aqueous organic redox flow batteries. *Nature Energy* **2018,** *3* (6), 508-514.

7.   Lin, K.; Gómez-Bombarelli, R.; Beh, E. S.; Tong, L.; Chen, Q.; Valle, A.; Aspuru-Guzik, A.; Aziz, M. J.; Gordon, R. G., A redox-flow battery with an alloxazine-based organic electrolyte. *Nature Energy* **2016,** *1*, 16102.

8.   Orita, A.; Verde, M. G.; Sakai, M.; Meng, Y. S., A biomimetic redox flow battery based on flavin mononucleotide. *Nat Commun* **2016,** *7*, 13230.

9.   Liu, Y.; Lu, S.; Chen, S.; Wang, H.; Zhang, J.; Xiang, Y., A Sustainable Redox Flow Battery with Alizarin-Based Aqueous Organic Electrolyte. *ACS Applied Energy Materials* **2019,** *2* (4), 2469-2474.

10.   Yang, Z.; Tong, L.; Tabor, D. P.; Beh, E. S.; Goulet, M.-A.; De Porcellinis, D.; Aspuru-Guzik, A.; Gordon, R. G.; Aziz, M. J., Alkaline Benzoquinone Aqueous Flow Battery for Large-Scale Storage of Electrical Energy. *Advanced Energy Materials* **2018,** *8* (8), 1702056.